Carbohydrate Polymers 83 (2011) 940–946

Contents lists available at ScienceDirect

Carbohydrate Polymers

journal homepage: www.elsevier.com/locate/carbpol

Fabrication of electrospun polycaprolactone biocomposites reinforced with chitosan for the proliferation of mesenchymal stem cells

Soongee Hong, GeunHyung Kim*

Bio/Nanofluidics Lab, Department of Mechanical Engineering, Chosun University, Gwangju 501-759, Republic of Korea

ARTICLE INFO

Article history:
Received 17 July 2010
Received in revised form 31 August 2010
Accepted 2 September 2010
Available online 9 September 2010

Keywords:
Chitosan
Polycaprolactone
Biocomposite
Mesenchymal stem cells

ABSTRACT

Biocomposites composed of poly(ε-caprolactone) (PCL) fibers and chitosan were obtained by two different fabrication methods: a two-step layer-by-layer technique and a co-electrospinning process. Fourier transform infrared spectroscopy and electron microscopy indicated that chitosan powders were embedded in the electrospun PCL mat. The resulting composites exhibited improved mechanical properties with an increase of about 75% in Young's modulus when compared with the pure PCL fiber mats. In addition, the fabricated biocomposites showed various synergistic effects including enhanced water absorption and hydrophilic properties. The biological response of mesenchymal stem cells (MSCs) on the biocomposites was superior to that on pure PCL in terms of improved cell attachment, higher proliferation, and morphological homogeneity. After 7 days of culture, cell proliferation was about 25% greater than on pure PCL. These observations suggest that chitosan-supplemented biocomposites would make excellent materials for tissue engineering applications.

1. Introduction

To regenerate damaged tissues, cells should be able to attach to, and proliferate in, a proper scaffold that can ultimately be implanted into the functioning tissue surrounding an injured area (Langer & Vacanti, 1993). In general, three different types of materials, including synthetic polymers, natural materials, (*e.g.*, collagen, chitosan, and alginic acid), and acellular tissue substitutes have been used for fabricating biomedical scaffolds (Yoon & Kim, 2010; Smith, Liu, & Ma, 2008). One of the synthetic polymers, poly(ε-caprolactone) (PCL), has been used for both soft and hard tissue regeneration. PCL has various advantages, including mechanical flexibility, low antigenicity, easy processability, and low degrees of chronic persistence (Glowacki & Mizuno, 2008). However, it can also cause problems related to its high hydrophobicity and low water absorptivity, toxicity, and low cell attachment and proliferation (Glowacki & Mizuno, 2008). To overcome these problems, composite materials composed of both synthetic and natural polymers, which are very similar to macromolecular substances that can be recognized and metabolized in a biological environment, have been proposed (Drury & Mooney, 2003; Yang, Zhu, Cui, Li, & Jin, 2009; Zhao et al., 2009).

One of the best-suited natural biopolymers, chitosan, has been considered an ideal tissue regeneration material because of its abundance, biocompatibility, biodegradability, and antibacterial and wound-healing activities (Kim et al., 2008). Chitosan is a linear polysaccharide, generally derived from the chitin found in crustacean exoskeletons, composed of glucosamine and N-acetyl glucosamine units linked by β(1–4) glycosidic bonds. The biocompatibility of chitosan makes it one of the most promising biomacromolecules for tissue engineered scaffolds and wound dressings (Zhou et al., 2008). However, the fabrication of nanofibers of pure chitosan is limited by high repulsive forces between ionic groups within the polymer backbone that arise during the application of a high electric field during electrospinning (Min et al., 2004). One plausible mitigation was described by Ohkawa, Cha, Kim, Nishida, and Yamamoto (2004), who obtained 330-nm chitosan fibers from a mixture of dichloromethane, chitosan, and trifluoroacetic acid. An alternative strategy involves the fabrication of composite materials. The typical composites are chitosan/poly(vinyl alcohol) (PVA) (Huang, Ge, & Xu, 2007), chitosan/poly(ethylene oxide) (PEO) (Kriegel, Kit, McClements, & Weiss, 2009), chitosan/poly(ethylene terephthalate) (PET) (Jung et al., 2007), and chitosan/poly(lactic acid) (PLA) (Peesan, Rujiravanit, & Supaphol, 2006). These composites exhibit several advantages over pure chitosan, including higher mechanical strength, biocompatibility, and antibacterial properties (Jayakumar, Prabaharan, Nair, & Tamura, 2010).

In general, an electrohydrodynamic process has been widely explored as a method to fabricate nanofibers for various biomedical applications, such as tissue-engineering scaffolds, wound dressing, drug-release systems, artificial organs and vascular grafts (Yoon & Kim, 2010). Additionally, recent novel methods, an electrohydrodynamic process to fabricate starch films (Pareta & Edirisinghe, 2006)

* Corresponding author. Tel.: +82 62 230 7180; fax: +82 62 236 3634.
E-mail address: gkim@chosun.ac.kr (G. Kim).

0144-8617/$ – see front matter © 2010 Elsevier Ltd. All rights reserved.
doi:10.1016/j.carbpol.2010.09.002

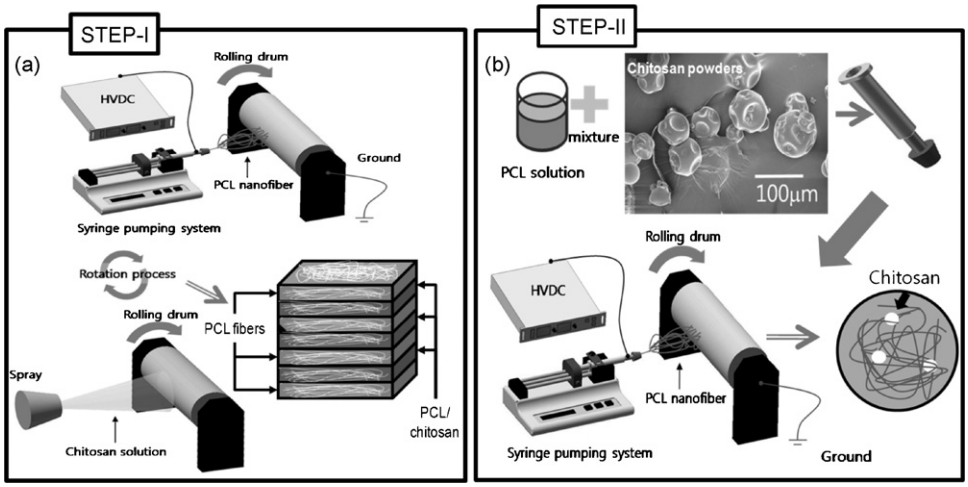

Fig. 1. Schematic illustrations of (a) the layer-by-layer fabrication of BC-1 biocomposites using normal electrospinning and air-spraying processes and (b) BC-2 biocomposite fabrication using a co-electrospinning process from a mixture containing PCL and chitosan powders (shown in the SEM micrograph).

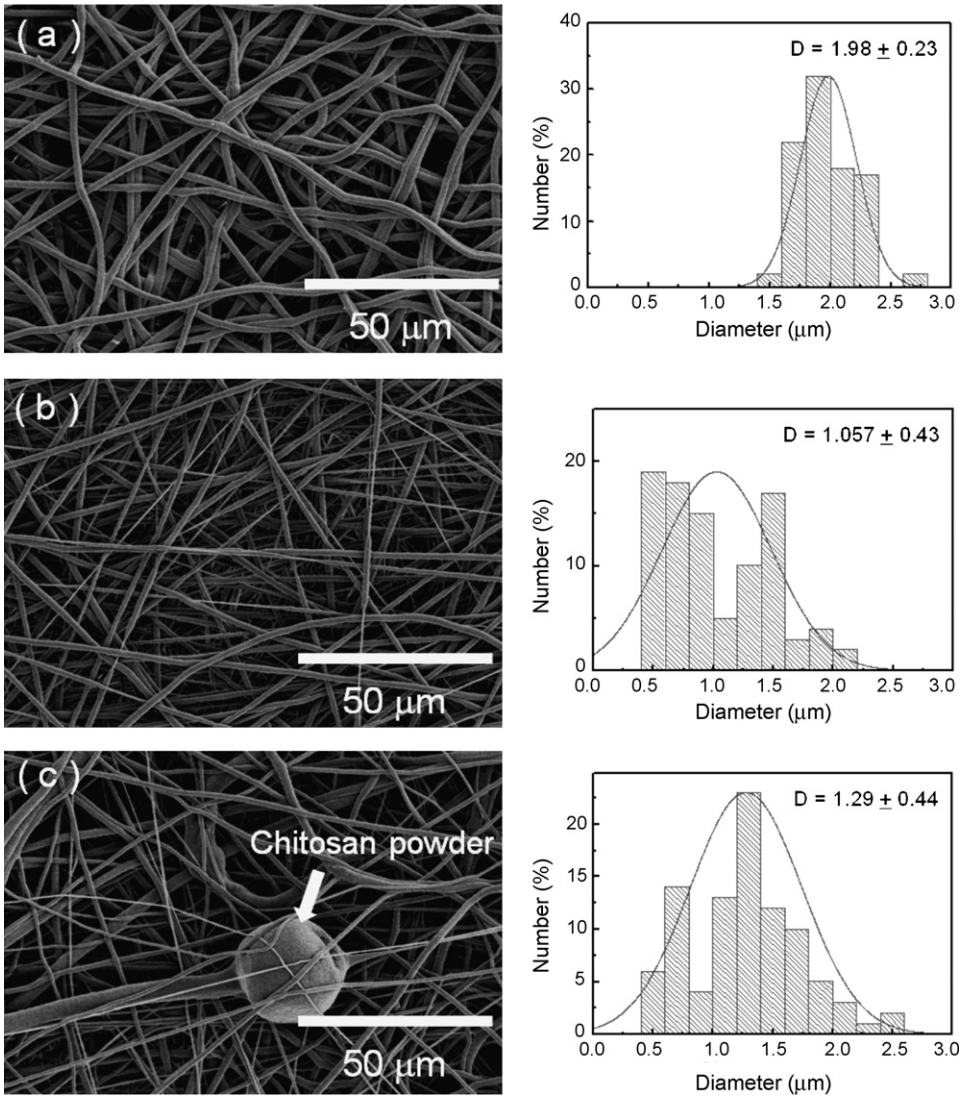

Fig. 2. Scanning electron micrographs of electrospun (a) pure PCL, (b) BC-1, and (c) BC-2. The histograms show the distribution of fiber diameters for each system.

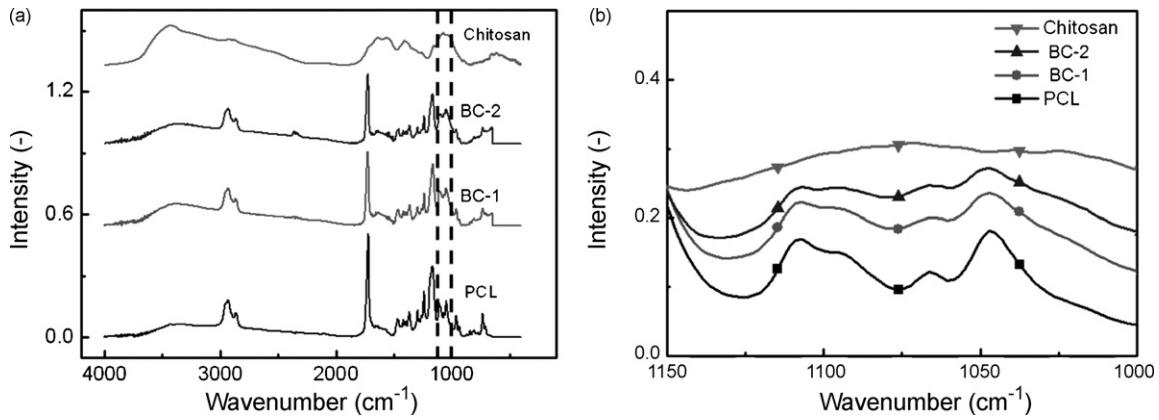

Fig. 3. (a) FTIR spectra of pure PCL, pure chitosan, and the BC-1 and BC-2 composites and (b) an enlargement of the spectra from 1150 to 1000 cm^{-1}.

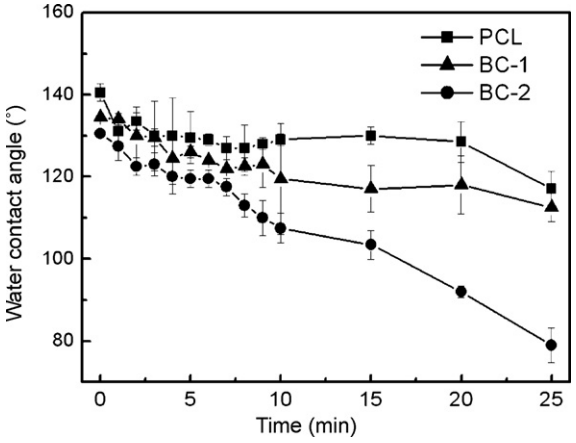

Fig. 4. A comparison of WCAs of pure PCL, BC-1, and BC-2 as a function of time.

and microbubble for targeted drug delivery (Stride & Edirisinghe, 2008) and electrohydrodynamic direct writing (Ahmad, Rasekh, & Edirisinghe, 2010) have been proposed for fabricating various functional biomaterials.

The current study describes two relatively simple processing methods for the fabrication of PCL/chitosan biocomposites, in which chitosan was used to reinforce electrospun PCL nanofibers. The first method describes the layer-by-layer deposition of electrospun PCL fibers and chitosan by an air-spraying process. The second method describes a co-electrospinning process in which a mixture of PCL and chitosan powders was electrospun in a single step. An auxiliary conical electrode was connected to the electrospinning nozzle to stabilize the electrospinning process. The PCL/chitosan biocomposites were characterized by measuring water contact angles, water absorption, and mechanical properties, as well as cell attachment and proliferation of mesenchymal stem cells (MSCs). The composites exhibited enhanced mechanical properties and improved hydrophilic characteristics and water absorption relative to pure PCL fiber mats. The biological response of MSCs on the biocomposites was also superior to that on pure PCL in terms of improved cell attachment, proliferation, and morphological homogeneity.

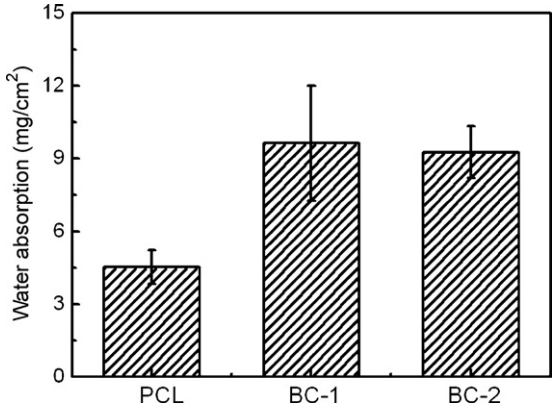

Fig. 5. Water absorption of PCL and the two biocomposite mats.

2. Experimental

2.1. Materials

PCL, with an average molecular weight (M_n) of 60,000 g/mol and a melting point of 60 °C, was obtained from Sigma–Aldrich (St. Louis, MO, USA). Electrospinning solutions were prepared with dimethyl formamide (DMF; Junsei Chemical, Tokyo, Japan) and methylene chloride (MC; Junsei Chemical) by mixing 80 wt% MC and 20 wt% DMF with 12 wt% PCL. Water-soluble chitosan (M_w = 200,000) was obtained from JAKWANG Inc. (Ansung-si, Gyeonggi-do, South Korea). Glutaraldehyde (25 wt%; Sigma–Aldrich) was used to cross-link the chitosan. Co-electrospun biocomposites were made from a solution containing 4 wt% chitosan powder and 12 wt% PCL, stirred for 24 h.

2.2. Biocomposite preparation

Fig. 1(a) and (b) illustrates the two different methods employed to fabricate PCL/chitosan biocomposites. Fig. 1(a) shows how layer-by-layer PCL/chitosan composites (BC-1) were obtained using general electrospinning and air-spraying techniques. First, a single layer of electrospun PCL fibers was deposited onto the rolling collector (1 m/s) for 10 min at an applied voltage of 18 kV (SHV300RD-50K power supply; Convertech, Suwon, South Korea). The feeding rate (1.5 mL/h) of the electrospun solution was controlled using a syringe pump (KDS 230; NanoNc, Seoul, South Korea). The distance between the needle tip and the collector was 15 cm. After fabricating the initial PCL microfiber mat, the chitosan solution, which was prepared in triply distilled water at a fixed concentration of 0.05 wt%, was air-sprayed onto the mat and allowed to dry for 12 h. The distance between the air-spraying nozzle and the mat was 15 cm. This procedure was repeated three times to obtain one PCL/chitosan biocomposite mat.

The co-electrospun PCL/chitosan biocomposite (BC-2) was electrospun onto a rolling collector from a solution containing 12 wt% PCL and 4 wt% chitosan powders (Fig. 1(b)). The total deposition

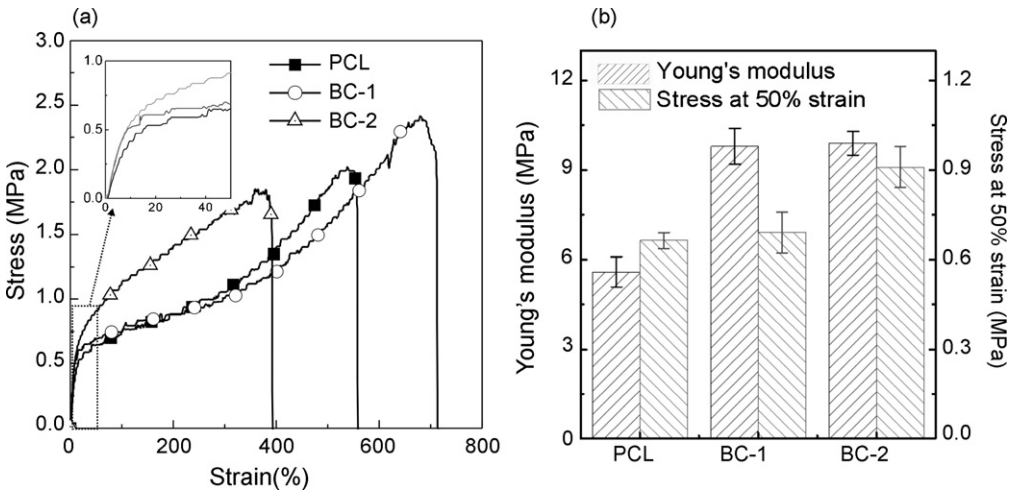

Fig. 6. (a) Stress–strain curves at a stretching rate of 0.5 mm/s and (b) Young's moduli and stress at 50% strain for the pure PCL mat and the two biocomposites.

time was 40 min. The applied voltage was 18 kV and the distance between the nozzle tip and the collector was 15 cm. The speed of the rolling collector was 1 m/s. In general, the processability of electrospun fibers is closely related to the electrical properties and surface tension of the injected solution. A homogeneous solution is desired. However, during electrospinning of the PCL/chitosan mixture, some sedimentation of chitosan powder was observed. This effect was minimized by using a conical electrode (0.2 mm thickness and 18.5 mm diameter) and by continuously stirring the mixture during electrospinning, which helped reduce the instability of the initial jet leaving the apex of the Taylor cone (Kim, 2006). These modifications resulted in a significantly more stable process than with a normal electrospinning system. BC-1 and BC-2 mats contained equivalent amounts of chitosan.

2.3. Biocomposite characterization

The mechanical properties of the biocomposites were characterized using a micro-tensile tester (Toptech 2000; Chemilab, Suwon, South Korea) in tensile mode on samples measuring 10 mm × 30 mm. Mechanical data were acquired in five independent experiments and all data are presented as mean values with a single standard deviation (SD). The sample thickness was measured at five different points under an optical microscope and the measured values were averaged. Samples were prepared parallel to the direction of rotation. Samples were stretched to failure at a rate of 0.5 mm/s at room temperature. The structural morphology of the electrospun biocomposites was observed under an optical microscope (BX FM-32; Olympus, Tokyo, Japan) connected to a digital camera and a scanning electron microscope (SEM; Sirion, Hillsboro, OR, USA). The diameter of the electrospun fibers in the composites was determined from SEM micrographs.

Infrared spectra were obtained from biocomposite mats and pure powders of chitosan and PCL using the attenuated total internal reflection (ATR) mode of a Fourier transform infrared (FTIR) spectrometer (Model 6700; Nicolet, West Point, PA, USA). Spectra represent the average of 30 scans between 400 and 4000 cm^{-1} at a resolution of 8 cm^{-1}.

Water absorption was calculated by weighing the composites before and after soaking in distilled water for 12 h in accordance with the methodology of Li et al. (2010). Prior to weighing, excess water was removed from the composites by gently blotting with filter paper. The composites were weighed on an AD-4 autobalance (Perkin-Elmer, Waltham, MA, USA).

Water contact angles (WCAs) were measured using a contact angle analyzer (Phoenix 300; Surface and Electro-Optics, Ansan, South Korea). Measurements were acquired at five independent points and are presented as the average value ± standard deviation (SD).

Electrical conductivity was measured using a multiparameter analyzer (model C861; Montreal Biotech Inc., Dorval, QC, Canada).

2.4. Cell culturing

Samples for cell culturing were prepared as 1.6-cm-diameter disks and sterilized using 70% ethanol and ultraviolet light prior to being placed in the culture medium overnight. MSCs were provided by JB Stem-cell Inc. (Hwasun, South Korea) and were cultured in Dulbecco's modified Eagle's medium (DMEM; Hyclone, Logan, UT, USA) supplemented with 10% fetal bovine serum (FBS; Hyclone) and 1% penicillin/streptomycin. The cells were maintained up to passage 14 and collected by trypsin–ethylenediaminetetraacetic acid treatment. The cells were then seeded on the composites at a density of 1×10^5 cells/sample and incubated in 5% CO_2 at 37 °C. The medium was changed every second day. The cell/composite constructs were fixed in 2.5% glutaraldehyde and dehydrated in a graded ethanol series. Cell growth was determined using an MTT [3-(4,5-dimethylthiazol-2-yl)-2,5-diphenyl tetrazolium bromide] assay (Cell Proliferation Kit I; Boehringer Mannheim, Mannheim, Germany). This assay is based on the principle that mitochondrial dehydrogenases in viable cells cleave the yellow tetrazolium salt MTT to produce purple formazan crystals. Cells on the biocomposite were incubated with 0.5 mg/mL MTT for 4 h at 37 °C; the absorbance of the surrounding solution was then measured at 570 nm with a microplate reader (EL800; BioTek Instruments, Winooski, VT, USA). Cell distribution in the biocomposites after a 7-day period was determined by incubating the cultured biocomposites with the actin-specific marker phalloidin-Alexa-568 (Invitrogen, Carlsbad, CA, USA) diluted 1:400 for 2 h at room temperature with shaking. The composites were then washed with 0.1 M phosphate-buffered solution containing 0.2% Triton X-100 and mounted with Vectashield (Vector Laboratories, Burlingame, CA, USA). Statistical analyses consisted of single-factor analyses of variance (ANOVAs). The significance level was set at $p < 0.05$.

3. Results and discussion

Fig. 2 shows scanning electron micrographs of a pure nanofiber mat (Fig. 2(a)) that was fabricated with a normal electrospinning

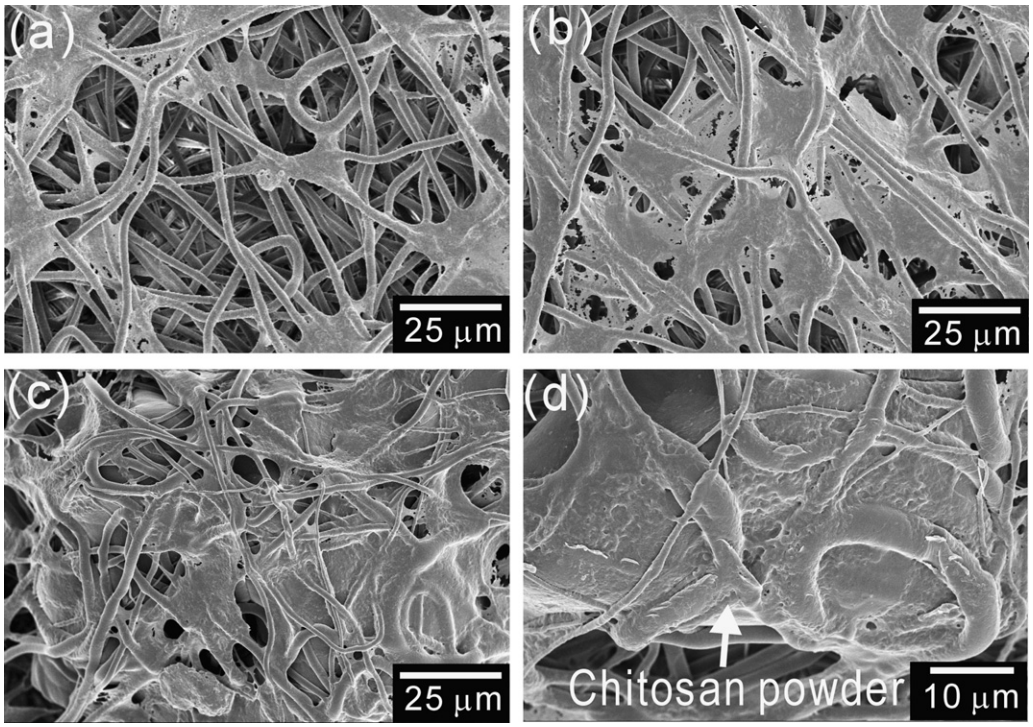

Fig. 7. SEM micrographs of MSCs cultured on (a) a pure PCL mat, (b) BC-1 and (c) BC-2 mats after 7 days of culturing. Cellular behavior on particles of chitosan powder within the BC-2 composite is shown in (d).

process, and biocomposites (Fig. 2(b) and (c)), fabricated via the layer-by-layer and co-electrospinning processes, respectively. The average diameters of PCL fibers in the pure PCL mat and in the BC-1 and BC-2 biocomposites were 1.98 ± 0.23 μm, 1.06 ± 0.43 μm, and 1.29 ± 0.44 μm, respectively. Differences in fiber diameter were likely due to differences in the conductivity of the electrospun solutions. The pure PCL solution had a conductivity of 2.1 μS/cm; the chitosan solution and mixtures of PCL/chitosan powders had conductivities of 2870 μS/cm and 4.7 μS/cm, respectively. In the layer-by-layer system, the electrospun PCL fibers were deposited on air-sprayed chitosan layers that had been coated onto previously deposited PCL fibers. This allowed one to vary the electric field between the nozzle and the coated PCL fiber with the chitosan mat as the target surface. According to Kim and Kim (2006), the surface resistance of the electrospinning target can influence the diameter of electrospun fibers. Therefore, the electric field between the nozzle and the chitosan-coated target in the layer-by-layer process likely decreased the diameter of the electrospun PCL fibers.

In the co-electrospun materials, the electrical conductivity of the PCL/chitosan mixture (4.7 μS/cm) was higher than that of the pure PCL solution (2.1 μS/cm). Therefore, repulsive forces between positive charges on the fiber surfaces will be higher. These forces allow the fibers to be stretched to a relatively greater extent during the electrospinning process and result in a decrease in the average fiber diameter.

The chitosan in the composites was cross-linked by immersion in a solution of 6 wt% glutaraldehyde in triply distilled water for 10 h at room temperature. Fig. 3(a) shows FTIR spectra of pure powdered chitosan, PCL, and the BC-1 and BC-2 biocomposites. The spectrum of pure PCL contains a strong peak around 1722 cm^{-1} corresponding to C=O stretching. The FTIR spectrum of pure chitosan shows several characteristic peaks, including N–H stretching vibrations at approximately 3352 cm^{-1}, and N–H bending transitions (Vieira & Beppu, 2006). The FTIR spectra in Fig. 3(b) indicate that chitosan was embedded within the composite mats.

The hydrophilicity of a material contributes significantly to initial cell attachment, proliferation, and migration (Rezwan, Chen, Blaker, & Boccaccini, 2006). To assess the effect of chitosan on the hydrophilicity of the composites, water contact angles (WCAs) were measured and compared to that of pure PCL. In general, since chitosan is relatively hydrophilic (WCA = 64°) (Cheng et al., 2003), the biocomposites would likely exhibit a higher hydrophilicity than the pure PCL mat. This hypothesis is confirmed in Fig. 4, where the WCA of a PCL electrospun mat is higher than that of the biocomposites. As shown in Fig. 4, the WCA of the PCL mat changed little, from 139° to 121°, after 25 min. In contrast, the WCAs of BC-1 and BC-2 decreased from 135° to 117° and from 131° to 79°, respectively,

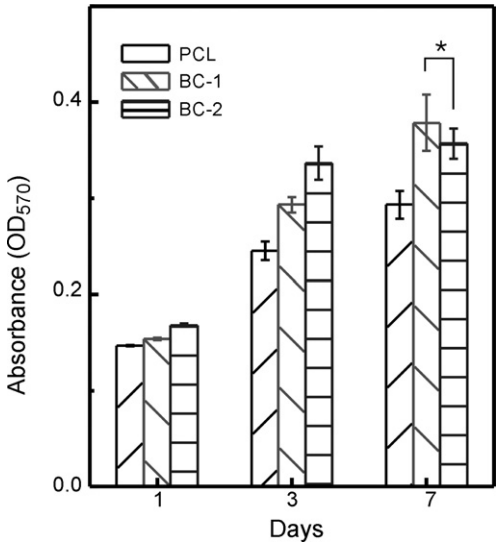

Fig. 8. Cell proliferation as indicated by an MTT assay of MSCs seeded on electrospun pure PCL and BC-1 and BC-2 composites. *$p < 0.05$ indicates a significant difference between BC-1 and BC-2.

over the same time period. The BC-2 composite exhibited a much greater change than the BC-1 composite. This result can be observed because the co-electrospun biocomposite (BC-2) has a more uniform distribution of chitosan powder throughout the thickness of the mat and at the mat surface, while the layering process used to fabricate the BC-1 composite did not result in a uniform distribution of chitosan. In addition, since the last step in the layer-by-layer process was the deposition of a PCL fiber mat, the top surface of the BC-1 composite was composed primarily of pure PCL fibers.

The water absorption of tissue engineering materials can influence cell proliferation and the structural morphology of the regrown tissue (Hollister, 2005). Fig. 5 shows the effect of chitosan content on the water absorption of the biocomposites. As indicated in the Fig. 5, the incorporation of chitosan increased water absorption by about 170% relative to that of the pure PCL scaffold. The degree of water absorption was similar for the two composites. This indicates that although the chitosan was inserted between the PCL fiber mats in BC-1, it was sufficiently exposed to attract a similar amount of water as in the BC-2 composite. The WCA and water absorption results both indicate that the chitosan in the biocomposites provided hydrophilic sites for water absorption. This would not only prevent the loss of bodily fluids and nutrients in *in vivo* tests, but would also increase the relatively low cell attachment and proliferation of pure PCL mats.

The mechanical properties of biomedical substitutes are important in providing physical support for cell growth and migration (Hollister, 2005; Murphy, Haugh, & O'Brien, 2010). Fig. 6 shows the stress–strain curves obtained from tensile tests of the PCL mat and the two biocomposites. The BC-1 and BC-2 biocomposites showed Young's moduli of 9.8 ± 0.6 MPa and 9.9 ± 0.4 MPa and stresses of 0.7 ± 0.06 MPa and 0.9 ± 0.07 MPa at 50% strain, respectively, while the pure PCL mat exhibited a Young's modulus of 5.6 ± 0.7 MPa and a stress of 0.6 ± 0.3 MPa at 50% strain. The Young's moduli of the biocomposites were analyzed using the modified Halpin–Tsai equation (Chou, Gao, Thostenson, Zhang, & Byun, 2010; Halpin & Kardos, 1976) shown below, which represents a simple approximation for predicting the modulus of particle-reinforced composites.

$$E_{COM} = \left[\frac{3}{8}\frac{1+0.67\zeta\phi}{1-\zeta\phi} + \frac{5}{8}\frac{1+2\xi\phi}{1-\xi\phi}\right] E_{PCL} \quad (1)$$

$$\zeta = \left[\frac{E_{Chi}/E_{PCL}-1}{E_{Chi}/E_{PCL}+0.67}\right], \quad \xi = \left[\frac{E_{Chi}/E_{PCL}-1}{E_{Chi}/E_{PCL}+2}\right] \quad (2)$$

In Eq. (1), E_{COM} and ϕ are the Young's modulus of the composite and the volume fraction of chitosan, respectively. E_{Chi} and E_{PCL} are the Young's moduli of chitosan and PCL. In Eq. (2), ζ and ξ are roughly unity because of the high modulus of chitosan compared with that of PCL. The Young's modulus of PCL is 4.9 MPa from previous tensile tests. The Young's modulus of chitosan powder is 906 MPa (Wu, Wan, Cao, & Wu, 2008). The equation further assumes that the shape of the chitosan particles was rectangular, as shown in the SEM micrograph in Fig. 1(b). According to Eqs. (1) and (2), the calculated modulus for both biocomposites was 9.6 MPa. Although assumptions were made regarding the shape of the chitosan particles, the dispersion uniformity of chitosan, and the surface interactions between the chitosan powder and the electrospun PCL fibers, the calculated value and measured values were similar. Furthermore, the modulus of BC-1 was similar to that of the BC-2. This phenomenon may be explained as follows. During stretching of the composite, the PCL matrix was the first to deform while the chitosan-coated PCL fibers, illustrated in Fig. 1(a), acted as a reinforcing bridge and increased the resistance to deformation. Note that while the stress at 50% strain was higher with the BC-2 composite, the maximum strain was much smaller than that of BC-1. This phenomenon is likely due to concentrated stresses in BC-2 as a result of chitosan powder aggregates.

The effect of chitosan on cell attachment and proliferation was evaluated by embedding MSCs in pure PCL, and in BC-1 and BC-2. In general, micro/nanofibrous materials are promising biomaterials for cell culturing and tissue engineering applications because the morphology of the fibers is very similar to that of native human extracellular matrix (Venugopal, Low, Choon, & Ramakrishna, 2008).

Fig. 7(a)–(c) show SEM micrographs of MSC proliferation 7 days after seeding on a pure PCL mat, and the BC-1 and BC-2 composites, respectively. MSCs spread across the surfaces of the two composites, while those on the PCL mat were sporadically distributed. This phenomenon may occur because the chitosan domains act as hydrophilic sites with high water absorption, thereby allowing cells to more easily attach and proliferate from these areas. This assumption is validated by the micrograph in Fig. 7(d), which shows that the chitosan powder in the composite materials was coated with cells.

The results of the MTT assay in Fig. 8 show that MSC proliferation increased on both PCL and both biocomposites as a function of time. In particular, significant differences between the PCL and composite mats were observed on days 3 and 7. These cell-culturing results show that PCL fiber mats processed with chitosan better promote cell propagation without any additional chemical treatment. Furthermore, the BC-1 composite, which is relatively simple to fabricate, exhibits a similar cellular response and mechanical behavior as the BC-2 co-electrospun composite.

4. Conclusions

PCL/chitosan composites were fabricated using two methods combining electrospinning and air spraying. The resulting composites exhibited improved mechanical properties with an increase of about 75% in their Young's moduli when compared with electrospun mats of pure PCL. In addition, the fabricated biocomposites showed various synergistic effects including enhanced water absorption and increased hydrophilicity. Cell culturing and SEM micrographs indicated that interactions between MSCs and the biocomposites were much more favorable than those between MSCs and scaffolds made from pure PCL. These results demonstrate that the inherent hydrophobicity of synthetic PCL can be modified by incorporating a small amount of chitosan. These fabricating methods and the resulting composites boast excellent mechanical and biological properties for biomedical applications.

References

Ahmad, Z., Rasekh, M., & Edirisinghe, M. (2010). Electrohydrodynamic direct writing of biomedical polymers and composites. *Macromolecular Materials and Engineering*, *295*, 315–319.

Cheng, M., Deng, J., Yang, F., Gong, Y., Zhao, N., & Zhang, X. (2003). Study on physical properties and nerve cell affinity of composite films from chitosan and gelatin solutions. *Biomaterials*, *24*, 2871–2880.

Chou, T. W., Gao, L., Thostenson, E. T., Zhang, Z., & Byun, J. H. (2010). An assessment of the science and technology of carbon nanotube-based fibers and composites. *Composites Science and Technology*, *70*, 1–19.

Drury, J. L., & Mooney, D. J. (2003). Hydrogels for tissue engineering: Scaffold design variables and applications. *Biomaterials*, *24*, 4337–4351.

Glowacki, J., & Mizuno, S. (2008). Collagen scaffolds for tissue engineering. *Biopolymers*, *89*, 338–344.

Halpin, J. C., & Kardos, J. L. (1976). The Halpin–Tsai equations: A review. *Polymer Engineering and Science*, *16*, 344–352.

Hollister, S. J. (2005). Porous scaffold design for tissue engineering. *Nature Materials*, *4*, 518–524.

Huang, X. J., Ge, D., & Xu, Z. K. (2007). Preparation and characterization of stable chitosan nanofibrous membrane for lipase immobilization. *European Polymer Journal*, *43*, 3710–3718.

Jayakumar, R., Prabaharan, M., Nair, S. V., & Tamura, H. (2010). Novel chitin and chitosan nanofibers in biomedical applications. *Biotechnology Advances*, *28*, 142–150.

Jung, K. H., Huh, M. W., Meng, W., Yuan, J., Hyun, S. H., Bae, J. S., et al. (2007). Preparation and antibacterial activity of PET/chitosan nanofibers mats using an electrospinning technique. *Journal of Applied Polymer Science*, *105*, 2816–2823.

Kim, G. H. (2006). Electrospinning process using field-controllable electrodes. *Journal of Polymer Science Part B: Polymer Physics*, *44*, 1426–1433.

Kim, G. H., & Kim, W. D. (2006). Nanofiber spraying method using a supplementary electrode. *Applied Physics Letters*, *89*, 013111.

Kim, I. Y., Seo, S. J., Moon, H. S., Yoo, M. K., Park, I. Y., Kim, B. C., et al. (2008). Chitosan and its derivatives for tissue engineering applications. *Biotechnology advances*, *26*, 1–21.

Kriegel, C., Kit, K. M., McClements, D. J., & Weiss, J. (2009). Eelectrospinning of chitosan-poly-(ethylene oxide) blend nanofibers in the presence of micellar surfactant solutions. *Polymer*, *50*, 189–200.

Langer, R., & Vacanti, J. P. (1993). Tissue engineering. *Science*, *260*, 920–926.

Li, X. Y., Kong, X. Y., Shi, S., Gu, Y. C., Yang, L., Guo, G., et al. (2010). Biodegradable MPEG-g-Chitosan and methoxy poly(ethylene glycol)-b-poly(ε-caprolactone) composite films: Part 1. Preparation and characterization. *Carbohydrate Polymers*, *79*, 429–436.

Min, B. M., Lee, S. W., Lim, J. N., You, Y., Lee, T. S., Kang, P. H., et al. (2004). Chitin and chitosan nanofibers: Electrospinning of chitin and deacetylation of chitin nanofibers. *Polymer*, *45*, 7137–7142.

Murphy, C. M., Haugh, M. G., & O'Brien, F. J. (2010). The effect of mean pore size on cell attachment, proliferation and migration in collagen–glycosaminoglycan scaffolds for bone tissue engineering. *Biomaterials*, *31*, 461–466.

Ohkawa, K., Cha, D., Kim, H., Nishida, A., & Yamamoto, H. (2004). Electrospinning of chitosan. *Macromolecular Rapid Communication*, *25*, 1600–1605.

Pareta, R., & Edirisinghe, M. (2006). A novel method for the preparation of starch films and coatings. *Carbohydrate Polymers*, *63*, 425–431.

Peesan, M., Rujiravanit, R., & Supaphol, P. (2006). Electrospinning of hexanoyl chitosan/po-lylactide blends. *Journal of Biomaterials Science, Polymer Edition*, *17*, 547–565.

Rezwan, K., Chen, Q. Z., Blaker, J. J., & Boccaccini, A. R. (2006). Biodegradable and bioactive porous polymer/inorganic composite scaffolds for bone tissue engineering. *Biomaterials*, *27*, 3413–3431.

Smith, L. A., Liu, X., & Ma, P. X. (2008). Tissue engineering with nano-fibrous scaffolds. *Soft Matter*, *4*, 2144–2149.

Stride, E., & Edirisinghe, M. (2008). Novel microbubble preparation technologies. *Soft Matter*, *4*, 2350–2359.

Venugopal, J., Low, S., Choon, A. T., & Ramakrishna, S. (2008). Interaction of cells and nanofiber scaffolds in tissue engineering. *Journal of Biomedical Materials Research Part B: Applied Biomaterials*, *84B*, 34–48.

Vieira, R. S., & Beppu, M. M. (2006). Interaction of natural and crosslinked chitosan membranes with Hg(II) ions. *Colloids and Surface A: Physicochemical and Engineering Aspects*, *279*, 196–207.

Wu, H., Wan, Y., Cao, X., & Wu, Q. (2008). Proliferation of chondrocytes on porous poly(DL-lactide)/chitosan scaffolds. *Acta Biomaterialia*, *4*, 76–87.

Yang, Y., Zhu, X., Cui, W., Li, X., & Jin, Y. (2009). Electrospun composite mats of poly[(D,L-lactide)-co-glycolide] and collagen with high porosity as potential scaffolds for skin tissue engineering. *Macromolecular Materials and Engineering*, *294*, 611–619.

Yoon, H., & Kim, G. (2010). Micro/nanofibrous scaffolds electrospun from PCL and small intestinal submucosa. *Journal of Biomaterials Science. Polymer edition*, *21*, 553–562.

Zhao, H., Ma, L., Gao, C., & Shen, J. (2009). Composite scaffold of PLGA microspheres/fibrin gel for cartilage tissue engineering: Fabrication, physical properties, and cell responsiveness. *Journal of Biomedical Materials Research Part B: Applied Biomaterials*, *88*, 240–249.

Zhou, Y, Yang, D., Chen, X., Xu, Q., Lu, F., & Nie, J. (2008). Electrospun water-Soluble carboxyethyl chitosan/poly(vinyl alcohol) nanofibrous membrane as potential wound dressing for skin regeneration. *Biomacromolecules*, *9*, 349–354.